Modeling the Effect of the Atmosphere on Light

R. VICTOR KLASSEN
University of Waterloo

The interaction of light with particles suspended in the air is the cause of some beautiful effects. Among these effects are the colors of the sunset, the blue of the sky, and the appearance of a scene in fog. A lighting model that takes into account the effects of scattering by suspended particles is presented. A method of computing the colors of the sun and sky, for any sun position above the horizon, is derived from the lighting model. The model is also suitable for rendering fog under general lighting conditions. As an example of the use of the model for rendering fog, the special case of fog lit by the sun, without shadows, is considered.

Categories and Subject Descriptors: I.3.3 [**Computer Graphics**]: Picture/Image Generation—*display algorithms*; I.3.7 [**Computer Graphics**]: Three-Dimensional Graphics and Realism—*color, shading, shadowing, and texture*

General Terms: Algorithms

Additional Key Words and Phrases: Fog, image synthesis, lighting interaction, natural sky simulation, scattering

1. INTRODUCTION

Realistic image synthesis has been given considerable attention over the last few years. Reflectance models such as that in [4], along with solid texturing [23] and normal perturbation [1] have contributed greatly to the beauty and variety of surfaces available. The use of ray tracing [25] made the simulation of reflecting and refracting surfaces possible. The interaction of multiple diffusely reflecting surfaces has been effectively modeled using the method presented in [11]. These techniques have modeled more and more effectively the interaction of light with surfaces in the environment, using the principles of ray optics and the conservation of energy.

Sometimes it is not sufficient to assume that light is traveling in a vacuum between surfaces. Where there are large amounts of dust or water vapor in the atmosphere, or where the distances are large enough that air molecules themselves have an effect, traditional ray tracing is ineffective. In some cases it is possible to use simple approximations that apply only to the special case in question. One

Author's address: Department of Computer Science, University of Waterloo, Waterloo, Ontario, Canada N2L 3G1.

example of this is fog, which has generally been rendered by varying the contrast as a function of distance [12, 26]. In this method the color of an object is averaged with a gray fog color. The fog color is weighted more and more heavily in the average as the object distance increases. Although this cannot produce the effect of a searchlight or of shadows in the fog, it has produced quite pleasing results at very little expense. The color of the sky has been produced using simple heuristics [7, 16] that are satisfactory in many instances, although unable to predict the color of the sun for a given sky. Blinn proposed a lighting model for clouds [2], which was used by Kajiya and Von Herzen to produce a number of images of clouds [13], but only white ones and only on a flat blue background.

In 1984 Max used Blinn's lighting model to light clouds [17], and to extend it to give the lighting of the haze beneath the clouds in the special case in which the sun shone from directly above, through holes in the cloud cover. His emphasis was on two special cases and not on the general problem. He restricted the geometry and applied certain approximations that allowed the computation to be performed in a reasonable amount of time on a CRAY-1.

In order to render correctly scenes in which large numbers of small particles have noticeable effects on the lighting, it is necessary to know what effect such particles have, and in which regions. Determining these regions is a nontrivial task, sometimes requiring ray tracing. We shall begin by describing a general lighting model for use in dispersive media, and then consider a number of cases that, due to the nature of their geometries, do not require ray tracing, but lend considerable justification to the model.

2. THE NATURE OF SCATTERING

Our primary interest is to model the effect of scattering by small particles suspended in the atmosphere. The intensity of scattered light about any particle forms a three-dimensional pattern, $\beta_{sc}^{(\lambda)}(\theta, \phi)$ (the angular scattering function), which depends on the size and shape of the particle, and on the wavelength λ of the light involved. Figure 1 shows the angles θ and ϕ for a single scattering event.

For spherical particles, and particles small enough to represent point discontinuities in the electric field experienced by the passing light, β_{sc} is symmetric about the line of propagation of the incident light, and so it is sufficient to write $\beta_{sc}^{(\lambda)}(\phi)$. This is the case for air molecules, water vapor (by virtue of their small average size), wet haze, and small raindrops (which are spherical). Nonspherical particles, large with respect to λ, are found in the air in dust storms and heavily polluted environments. The general lighting model that we give here is sufficient to handle such cases, given an appropriate scattering function, but approximations we use in the treatments of special cases will depend on the nature of the scattering function.

For small particles, of a radius less than about 0.05λ, Rayleigh scattering, named after Lord Rayleigh, who was the first to study it [24], predominates. This has a total angular scattering function proportional to $(1 + \cos^2\phi)/2$ [19].

Larger particles, of a size up to about the wavelength of the light, scatter more light, concentrating it in the forward direction. Still larger particles show extreme concentration of light in the forward lobe, with maxima and minima developing to the sides. The positions and numbers of the side lobes vary rapidly with the

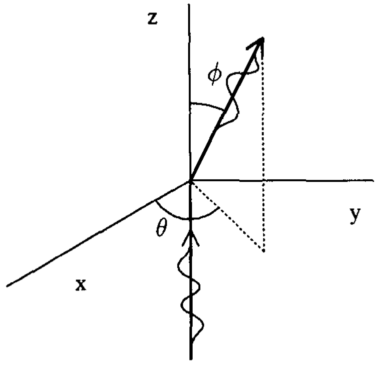

Fig. 1. Scattering angles for a single scattering event. The incoming ray is traveling in the positive z direction and is scattered at the origin.

size of the particle, and since the size of particles in the atmosphere is distributed over a continuum, their effect is negligible in the average [19]. Several examples of angular scattering functions are shown in Figure 2.

Complete tabulations of angular scattering functions for spheres may be found in [6]. These were calculated using a theoretical model developed by Mie [21]. Blinn has suggested [2] that the angular scattering function be approximated with

$$\frac{(1 - g)^2}{(1 + g^2 - 2g\cos(\phi))^{3/2}}. \tag{1}$$

The parameter g may be varied to cause the majority of light to be scattered either forward or backward. The value Blinn suggested for dust is appropriate for materials in which the majority of light is backscattered. No value was suggested for water droplets, and the reader is left to assume that the same value may be used. A careful examination of the beam of light caused by automobile headlights on a foggy night, viewed from various angles, will show that the majority of light is scattered forward, as with the scattering functions shown above. If the scattering function suggested by Blinn is used, then care should be taken to get the direction correct. We prefer to work with tabulated values, for speed.

The phrase *total scattering* refers to the total amount of light scattered from the beam (in all directions, as a fraction of the original intensity).

The scattering cross section, σ_{sc}, of a particle, which is not, in general, the same as the geometric cross section, gives the total amount of light scattered by an individual particle per unit incident irradiance. The scattering efficiency factor, Q_{sc}, is the ratio of the geometric cross section to the scattering cross section. This has considerable variation, as shown in Figure 3.

Rayleigh particles (particularly air molecules) show a high degree of selectivity, with the amount of scattering being inversely proportional to the fourth power of wavelength, whereas particles significantly greater in size than the wavelength of the light show no selectivity at all. For large particles, Q_{sc} becomes more nearly proportional to λ^{-2}, until particle size nears $\lambda/2$, at which it levels off at 2 after some oscillation.

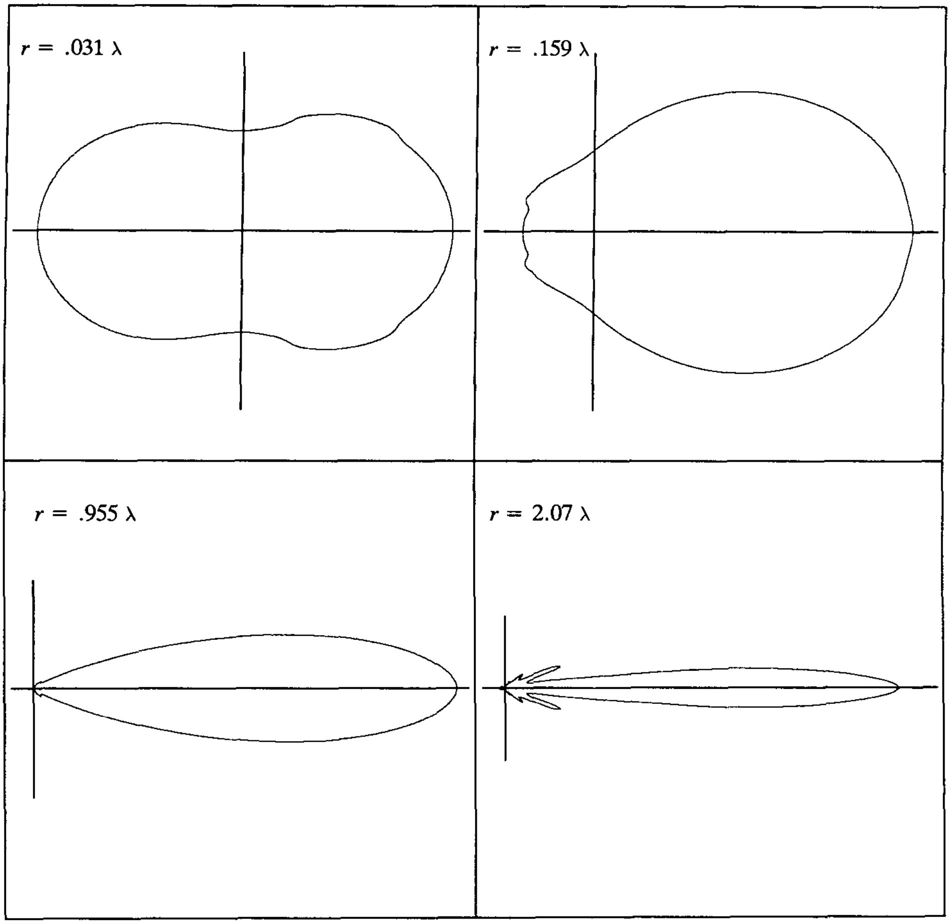

Fig. 2. Polar plots of angular scattering functions for spheres of water. Incident light is from the left and scattered at the origin. As droplet size increases, more and more of the light is scattered forward. The radial scales differ from the first to the last by a factor of 10^9. The data are from [6].

Although theoretical models do exist for the total scattering efficiency of small spheres, tabulations of experimentally observed values may be found in [19, Appendixes I and J], and they are sufficiently precise for our purposes. It was from there that the data for Figure 3 were obtained. Since a natural haze consists of particles of sizes distributed over a continuum, the fine structure on the curve of Figure 3 has no effect on the optical properties of real haze, and the effect of the large oscillations is less than it might appear [19].

It is useful to define an extinction coefficient, $\beta_{ex}^{(\lambda)}$, which gives the total amount of light lost from the beam per unit distance and depends on both the scattering cross sections of the particles and the density of particles along the path of the beam.

If particles in the scattering medium have an extinction coefficient $\beta_{ex}^{(\lambda)}$, then in a differential segment of the beam of length dx, where the intensity is $I(\lambda)$,

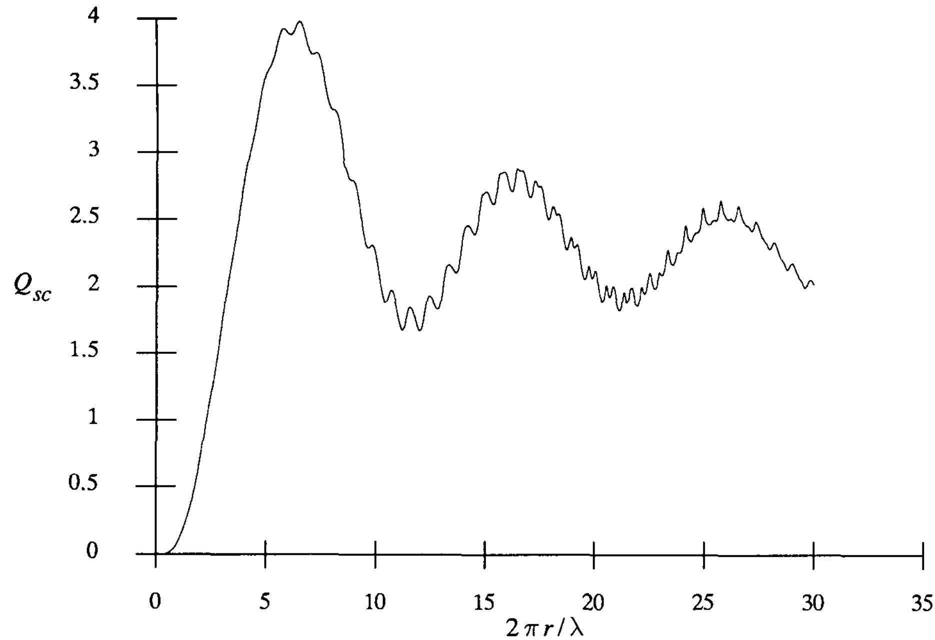

Fig. 3. Scattering efficiency of wet haze.

the amount lost from the beam is

$$dI(\lambda) = \beta_{\text{ex}}^{(\lambda)} I(\lambda)\,dx. \tag{2}$$

By integrating eq. (2) once for each wavelength sampled, the spectral intensity distribution of a beam with original intensity I_0 after traveling a distance r through the medium is found:

$$\int_{I_0}^{I_f} \frac{dI}{I} = \beta_{\text{ex}}^{(\lambda)} \int_0^r dx, \tag{3}$$

$$I_f = I_0 \exp(-\beta_{\text{ex}}^{(\lambda)} r). \tag{4}$$

From eq. (4) we may derive the transmittance T and opacity O of a given thickness of a medium of known scattering properties:

$$T = \frac{I_f}{I_0} = \exp(-\beta_{\text{ex}} r), \tag{5}$$

$$O = 1 - T = 1 - \exp(-\beta_{\text{ex}} r). \tag{6}$$

3. METHODS FOR MODELING SCATTERING

We now consider the path of a typical ray of light from a source to the eyepoint. It is assumed that the majority of light is scattered once. Figure 4 shows the path a typical ray might take. The transitions from one medium to another are modeled as sharp discontinuities. Although the justification for this assumption is not always satisfactory, it has not been found to produce any artifacts. Given

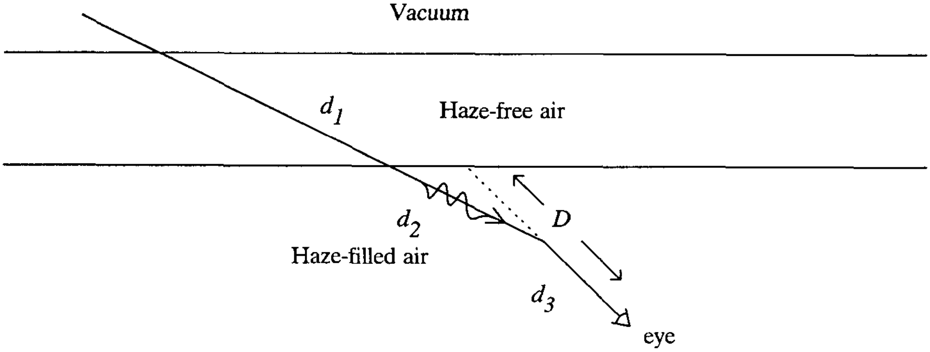

Fig. 4. The path of a typical ray.

these assumptions, light travels a distance d_1 through the atmosphere before entering the haze, and then travels a distance d_2 further before being scattered. If it is scattered exactly once, then the chance that it is scattered before it reaches the haze is very slight. After being scattered it travels a distance d_3 through the haze before reaching the eye. This last distance can vary from 0 to D.

Either D or d_1 may be zero: A value of zero for d_1 indicates a source within the haze or fog; a value of zero for D indicates an absence of haze or fog. If both are zero, the problem reduces to ray tracing in a vacuum. In the general case, neither is zero.

Consider then the general path. Light begins traveling through the atmosphere with an intensity vector I_0. As it travels along its path, it is attenuated by both haze and air. In the case of sunlight traveling through the atmosphere, the effect of haze is negligible at altitudes above 8–16 km, whereas molecular scattering has some effect at altitudes as high as 100 km. After traveling a distance d_1, it enters a region with an increased density of scattering particles. For the sake of discussion, let us say it enters the haze layer (in the case of a source with altitude less than 16 km, $d_1 \equiv 0$). By this point the intensity is

$$I_1 = I_0 \exp(-\beta^{(\lambda)}_{\mathrm{ex}_\mathrm{m}} d_1). \tag{7}$$

The subscript m on β_{ex} indicates molecular scattering. From now on we shall drop the superscript from β_{ex}, keeping in mind that it is wavelength dependent.

After traveling a distance d_2 through the haze, some of the light is scattered toward the viewer, scattering at an angle ψ. Before scattering, the intensity is

$$I_2 = I_1 \exp(-(\beta_{\mathrm{ex}_\mathrm{m}} + \beta_{\mathrm{ex}_\mathrm{p}})d_2). \tag{8}$$

Here the subscript p indicates scattering by particles. Of I_2 only a fraction $\beta^{(\lambda)}_{\mathrm{sc}}(\psi)$ is scattered toward the eye. The intensity leaving the scattering center in the direction of the eye is

$$I_3 = I_2 \beta^{(\lambda)}_{\mathrm{sc}}(\psi). \tag{9}$$

Finally, a portion of the beam is lost on its way to the eye, yielding

$$I_4 = I_3 \exp(-(\beta_{\mathrm{ex}_\mathrm{m}} + \beta_{\mathrm{ex}_\mathrm{p}})d_3) \tag{10}$$

after traveling a distance d_3. Substituting back and grouping terms yields

$$I_4 = I_0 \beta_{sc}^{(\lambda)}(\psi) \exp(-\beta_{ex_m} d_1 - (d_2 + d_3)(\beta_{ex_m} + \beta_{ex_p})). \tag{11}$$

This gives the amount of light arriving at a point from one path. Light reaching a given point from one direction comes from many paths all of whose last segments are collinear: For a given direction, the scattering event could occur anywhere along a line in that direction. To find the total amount reaching a point from a given direction, it is necessary to integrate over all possible values of d_3.

$$I = I_0 \beta_{sc}^{(\lambda)}(\psi) \int_0^D \exp(-\beta_{ex_m} d_1 - (d_2 + d_3)(\beta_{ex_m} + \beta_{ex_p}))\, dd_3. \tag{12}$$

The amount of light striking the final segment, and potentially being scattered, is proportional to the sine of the scattering angle, that is, the angle between the final segment and the previous one. For a distributed source such as the sun, the angle will not be defined as a single value, but must be treated as varying from one extreme to the other. The sin ψ term that is produced from these considerations may be absorbed into $\beta_{sc}^{(\lambda)}(\psi)$, so that the expression of eq. (12) is unchanged.

For some simple geometries, this integral may be found symbolically beforehand; in general, it requires numerical evaluation. Because it must be evaluated for each of the wavelengths sampled, symbolic evaluation is by far the preferred approach wherever it can be done.

The integral of eq. (12) only gives the contribution of the haze or fog to the light for one line of sight or reflection; this contribution must be combined with any other contributions, such as the light reflected by some object partially obscured by the haze or fog, taking into account the opacity of the haze as given by eq. (6).

4. THE COLOR OF THE SUN AND THE SKY

In the absence of all dust and moisture in the atmosphere, the sky would have a color very nearly a constant blue, that color being the additive mixture of all the wavelengths represented in the solar spectrum, each weighted by the fraction of that wavelength scattered.

Both the color of the sun and that of the sky are at least partially a result of Rayleigh scattering. The effect of haze in the atmosphere is also important in determining the color of the sky, even at times when the sun is not at all obscured by haze, as it lends the whitish color to the horizon at noon.

A good approximation for the spectral distribution of sunlight as it enters the atmosphere may be found in [9].

The color and intensity of sunlight are determined by the initial color and intensity, reduced by the effects of scattering along the path. The path of a typical ray is shown in Figure 5, in which refraction has been neglected. Refraction only plays a significant role when the sun is near the horizon. Even then the bending is not more than a few degrees [19].

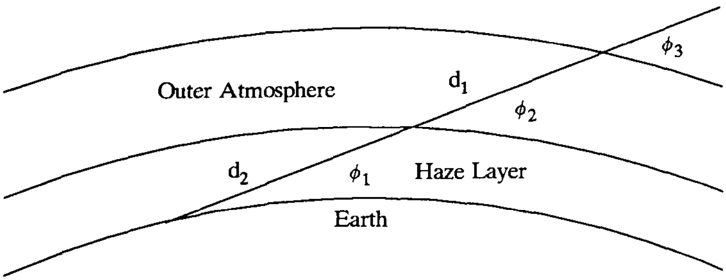

Fig. 5. The path of a ray from the sun.

The remaining effect of the atmosphere on the light from the sun is partial extinction, particularly of the short wavelengths. From eq. (4) we know that, if the light travels a distance d_1 through the atmosphere before striking an appreciable amount of haze, and then travels a distance d_2 through the haze, the final intensity will be

$$I^{(\lambda)} = I_0^{(\lambda)} \exp(\beta_{\mathrm{ex}_\mathrm{m}}(d_1 + d_2) + \beta_{\mathrm{ex}_\mathrm{p}} d_2). \tag{13}$$

Here I_0 gives the spectral distribution of light entering the atmosphere.

Note that, in the diagram (Figure 5), the angles, ϕ_i, at which the ray crosses the arcs differ. A careful analysis shows that, for radii such as that of the earth, they differ most for $\phi_1 = 0$, for which $\phi_3 = 10°$. Such a small error makes little difference in the calculations of the colors of the sun and sky.

5. THE COLOR OF THE SKY

The color of the sky found on a given line of sight depends both on the amount of scattering into that line of sight and the color of the light scattered. To simplify matters we shall assume single scattering. The blue color of the sky, that due entirely to Rayleigh scattering, will be modeled as a constant color throughout the sky. This leaves only the color being scattered by haze particles along the line of sight. The spectral intensity distribution of scattered light depends on the color of the light incident on the line of sight, and the angle of scattering.

Ignoring refraction we find that, for any angle of inclination of the sun, the angle between the line of sight and a line to the sun is effectively the same at all those points along the line of sight that are much closer to the viewer than to the sun. This follows immediately from the approximation of parallel rays from a distant light source.

6. GEOMETRY OF THE SKY

To compute each of the distances d_1–d_3, we need to find the distance along a ray from one sphere to a concentric one, in which the ray has an arbitrary direction, but is known to intersect both spheres. The direction of the ray is given by the angle it makes with the tangent plane of the inner sphere, since the distance depends only on this angle and the respective radii. For the first distance, d_1, the inner sphere is the edge of the haze layer, and the ray direction is the propagation

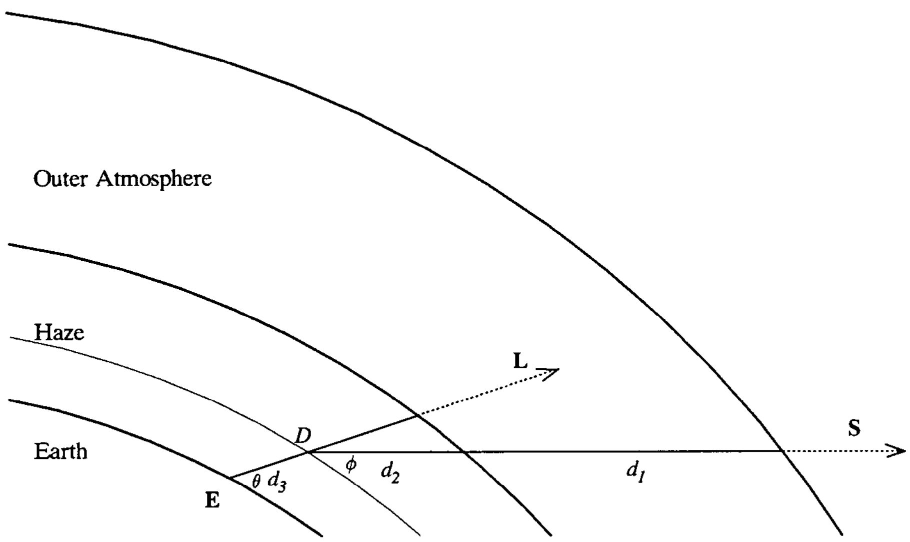

Fig. 6. The path of a typical ray, and the distances involved. The observer is at E, looking in the direction L. The sun direction is S. Light travels a distance d_1 through the outer atmosphere before reaching the haze. It then travels a distance d_2 before being scattered and d_3 after. d_3 varies from 0 to D.

direction of light from the sun. For the second distance, d_2, the ray direction is the same; the inner sphere passes through the scattering point, while the outer sphere is the same as the inner sphere for the first distance, although, if the observer were above the surface, it would be a sphere concentric with the earth and passing through the observer. The third distance, d_3, is computed with the ray along the line of sight, but a new inner sphere, this time the surface of the earth. Again, the outer sphere is the same as the inner sphere for the previous distance. Figure 6 shows the rays and spheres (projected into two dimensions) for these computations. The radius of the atmosphere has been artificially increased for visibility.

To compute any of the relevant distances, we use the construction of Figure 7. Here only two concentric spheres are indicated rather than three. As we shall see, each of the distances d_1–d_3 required in the lighting model may be obtained through an appropriate substitution of values into the radii and angles shown. The distance $d_i(r)$ is in each case given by y.

Suppose light enters the atmosphere at an angle of ϕ with the horizontal. Before entering the haze layer, it travels a distance y through the atmosphere, taking r to be R_H (the radius of the haze layer), and R to be R_A (the effective radius of the atmosphere). The atmosphere does not have a uniform density, nor does it simply drop off exponentially as the simplest models assume. Fortunately the distance always appears multiplied by the density in the formulas giving the amount of light scattered or lost from the beam. By reducing the radius of the atmosphere appropriately, we may approximate the effect of the variance in density, without actually modeling it.

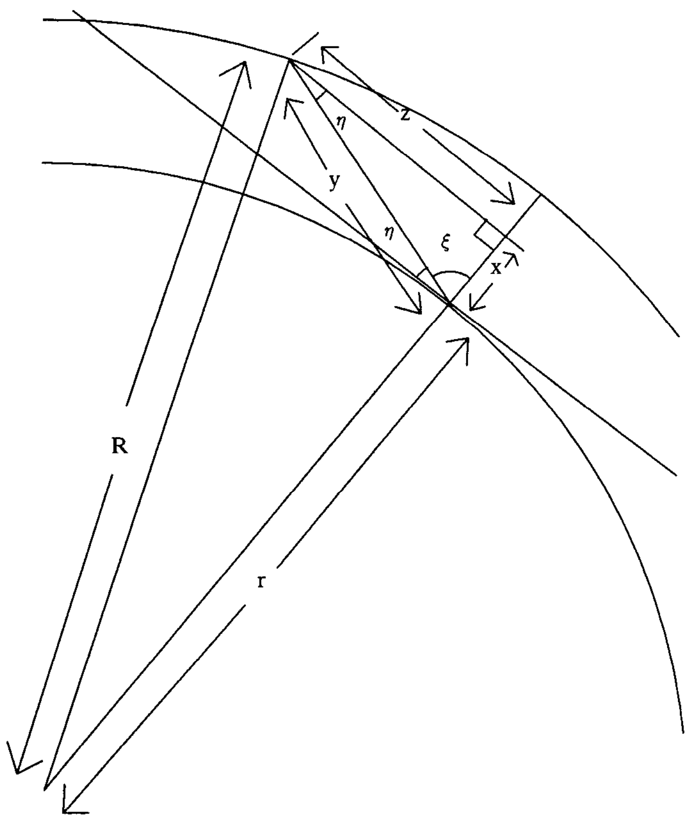

Fig. 7. The geometry of the sky.

Next consider the distance the light travels through the haze before scattering. If R is taken as R_H, and r is allowed to vary from R_E to R_H, then y gives this distance.

Finally the distance traveled after scattering (through haze and atmosphere) may be found by changing the angle ϕ to that of the angle θ between the line of sight and the horizontal, and letting R vary as r did in the previous instance, while r is fixed at R_E, the radius of the earth.

What remains is to find y in terms of R, r, and ϕ. We construct the right triangle of Figure 7, the length of whose hypotenuse is y.

By Pythagoras's theorem

$$(r + x)^2 + z^2 = R^2. \tag{14}$$

From the law of sines

$$z = x \tan \xi, \tag{15}$$

$$x = y \cos \xi. \tag{16}$$

Substituting for z from eq. (15) into eq. (14) gives

$$(r + x)^2 + x^2\tan^2\xi = R^2. \tag{17}$$

Substituting for x from eq. (16) into eq. (17) and expanding yields

$$r^2 + 2yr\cos\xi + y^2\cos^2\xi + y^2\cos^2\xi\tan^2\xi = R^2. \tag{18}$$

Solving for y,

$$y = \sqrt{R^2 - r^2\cos^2\phi} - r\sin\phi \tag{19}$$

in which the positive square root has been taken to yield a positive distance.

7. COMPUTING THE COLORS OF THE SUN AND SKY

Knowing the distance y of Figure 7, the three distances required for computing the color of the sky and the two needed for the color of the sun may be found by substituting in values for the angles and radii.

We begin with the color of the sun. To find d_1, recall the geometry of Figure 7 and eq. (19). Substitute R_A for R, and the angle of inclination of the sun for ϕ, and

$$d_1 = \sqrt{R_A^2 - R_H^2 cos^2\phi} - R_H\sin\phi. \tag{20}$$

Similarly for d_2, use the same equation with R_H replacing R, and R_E in the place of r:

$$d_2 = \sqrt{R_H^2 - R_E^2\cos^2\phi} - R_E\sin\phi. \tag{21}$$

This gives a final intensity of

$$\begin{aligned} I^{(\lambda)} = I_0^{(\lambda)}\exp(\beta_{\mathrm{ex}_p}(\sqrt{R_H^2 - R_E^2\cos^2\phi} - R_E\sin\phi) \\ + \beta_{\mathrm{ex}_m}(\sqrt{R_A^2 - R_H^2\cos^2\phi} + \sqrt{R_H^2 - R_E^2\cos^2\phi} - R_H\sin\phi - R_E\sin\phi)). \end{aligned} \tag{22}$$

The color of the sky is somewhat more difficult to compute. Recalling eq. (9) we substitute in the values for the angles and radii and integrate.

$$I_4 = \int_0^{l_{\max}} I_0\beta_{\mathrm{sc}}^{(\lambda)}(\psi)\exp(-\beta_{\mathrm{ex}_m} d_1(r) - (d_2(r) + d_3(r))(\beta_{\mathrm{ex}_m} + \beta_{\mathrm{ex}_p}))\, dl, \tag{23}$$

$$d_1 = \sqrt{R_A^2 - R_H^2\cos^2\phi} - R_H\sin\phi, \tag{24}$$

$$d_2(r) = \sqrt{R_H^2 - r^2\cos^2\phi} - r\sin\phi, \tag{25}$$

$$d_3(r) = \sqrt{r^2 - R_E^2\cos^2\theta} - R_E\sin\theta. \tag{26}$$

Here θ is the angle of inclination of the line of sight, while ϕ is that of the line to the sun.

The integral to be performed is a path integral in which the distance along the path may be found from

$$l(r) = \frac{l_{\max} r}{R_H - R_E} - l_{\max} R_E, \tag{27}$$

$$dl = \frac{l_{\max}}{R_H - R_E}\, dr. \tag{28}$$

With the change in variable given by eq. (28), the limits of the integral become R_E and R_H. The final expression for the intensity of the haze is then

$$I^{(\lambda)} = \frac{l_{max}}{R_H - R_E} I_0 \beta_{sc}^{(\lambda)}(\psi) \exp(-\beta_{ex_m} d_1) \times \int_{R_E}^{R_H} \exp(-(d_2(r) + d_3(r))(\beta_{ex_m} + \beta_{ex_p}))\, dr. \tag{29}$$

The upper limit in eq. (23) is the distance along the line of sight to the outer edge of the haze layer:

$$l_{max} = \sqrt{R_H^2 - R_E^2 \cos^2\theta} - R_E \sin\theta. \tag{30}$$

From eq. (6) and the definition of l_{max}, the opacity of the haze layer is simply

$$O = 1 - \exp(-\beta_{ex_p} l_{max}). \tag{31}$$

With the color and opacity of the haze layer computed, they may be combined with the underlying blue sky yielding the actual color of the sky. The underlying color of the blue sky changes little in spectral distribution during the course of a day; however, the brightness of a clear sky changes by a factor of 100 from noon to sunset, and very quickly drops from then on.

Since the color itself does not change, it may be computed once for a typical sky or estimated by eye. The eye is very forgiving with regard to variations in absolute color, but much more demanding of correct relative colors; hence the base color of the sky is of little importance, as long as it is a reasonable shade of blue.

8. EFFICIENCY CONSIDERATIONS

As presented thus far, computing the color of a single pixel, that is, the color along one line of sight, can require over 1 s of VAX 11/780 processing time. We have chosen to sample the intensity at 33 wavelengths, taking samples at 10-nm intervals. This choice is based on the fact that the eye can discriminate hues at approximately that resolution. In the interests of efficiency, one might consider converting the scattering coefficient vectors, and the incident intensity vector, to a three-coordinate color space, such as CIE XYZ or RGB, before performing such costly operations as the integration. This is *not* recommended. Although it does reduce the cost of computing a single image by a factor of 11, this is not a change in complexity, nor does it yield correct results. The nonlinearity of the integrand implies that the operations of evaluating the integral and changing color spaces do not commute.

A simple example shows why this is the case. Ignore for the moment all but molecular scattering, and also suppose the line of sight is directed high enough that the curvature of the earth does not play a role in determining the distances involved. Then the integral is simply

$$\int_0^{l_{max}} \exp(-\beta_{ex} m r)\, dr \tag{32}$$

with solution

$$\frac{1 - \exp(-\beta_{ex} m l_{max})}{\beta_{ex} m}, \tag{33}$$

where m depends on the slope of the line of sight. Since the components of the scattering coefficient vector are all positive, the argument to the exponential function is negative, so the result is between zero and one. This is multiplied by the intensity vector of the sunlight and added to the blue color of the sky to give the final color. At no point are any colors negative. Now suppose that the scattering coefficients were converted into a three-component color space. Because scattering is so much stronger in the blue, one or more of the coefficients will be negative. This means that the result of exponentiation will be greater than one, and the color will be negative. There is no guarantee that when this is added to the blue the resulting color will have only positive components.

A much better method of reducing the cost of the algorithm uses spatial coherency to make the cost of the algorithm less than $O(n \times m)$ for any reasonable values of m and n, the height and width of the image.

In a raster representation with finite precision representations for the colors, there will generally be large spans of constant color. In order to avoid computing neighboring pixels of the same color, the parameters may be checked (particularly the viewing angle) before the integral is performed. If the angle has not changed more than some small threshold, the integral need not be performed. Since integration is the dominant cost, reducing the number of integrations by any factor will reduce the total run time by nearly the same factor.

The threshold may be selected based on the number of bits of precision the final colors will have. The complexity is reduced for such image sizes in which the cost of the function calls continues to dominate the cost of writing the output, since an increase in resolution will increase the separation of pixels with sufficiently different view angles, leaving the number of calls roughly constant. This has reduced run time from an hour for a 128×64 image to a few minutes, with no visible loss of fidelity when the image was displayed on a frame buffer with 8 bits for each of red, green, and blue.

The size of an acceptable threshold decreases with increasing image complexity: This method makes images that should be really inexpensive to compute quite cheaply, but has less effect on expensive images. A sunset is much more expensive than a noon sky since the amount of red in the color of the sky varies more quickly, so the color must be reevaluated more often to prevent Mach bands in the sky.

We have found it most useful to do our integration using adaptive Simpson quadrature [3]. The depth of integration varies significantly with the angles of inclination of the line of sight and the sun. In order to further save time, the integrator returns its previous result if the first-order result is close to that from the previous call.

With these optimizations, the color of the sky was computed at a number of resolutions, up to 512×256. Table I shows the running times, in VAX 8600 CPU seconds. Note that the total time grows more slowly than linearly with the number of pixels.

Table I. Comparative Running Times for Sky Computations

Pixels	Seconds	Seconds per pixel
Noon		
131,072	153	0.0011673
32,768	60	0.00183105
8,192	25	0.00301514
2,048	11	0.00522461
512	5	0.0105469
128	3	0.0203125
Sunset		
131,072	654	0.00498962
32,768	309	0.00942993
8,192	144	0.0175781
2,048	64	0.03125
512	31	0.0613281
128	13	0.101563

A cruder method of reducing the time required to produce an image is to render at a low resolution and scale the image up as a postprocess. Because sky colors vary particularly smoothly, they lend themselves readily to this technique as well. Even a sky is not smooth enough to be scaled up very far by simple pixel replication, so a more sophisticated technique is needed. Such a technique, using B-splines to represent the red, green, and blue components of the image, has been developed, and is presented in [15].

No reasonably accurate method is known to date that is able to produce a background sky quickly. For this reason it is preferred to precompute a sky and store it, either at a low resolution to be later expanded, or at a high resolution to be used directly. Such an image, computed separately from the remainder of the scene, may be reused for a large number of scenes, with the cost of the initial computation amortized over time.

Since sky colors vary little horizontally, a background image of the sky will compact well under run-length encoding. A single background sky is often sufficient for several minutes of animation, as long as the direction of view does not change. For an animated sequence in which there is camera motion, one image could be stored per camera direction. The (space) cost of doing so is reasonable if the data are run-length encoded.

Figures 8–10 show the effect of varying the density and radius of the haze layer, and the mean density of the atmosphere, at sunset. Figure 11 shows the effect of variations of the haze density when the sun is inclined 40° from the horizon. In these four plates the numbers in the frames are intended as indications of relative values only. Figures 12 and 13 show a progression of sky colors in which the solar inclination is varied with all else held fixed. Where the sun is low in the sky, the entire image has been brightened, as if the camera aperture had been increased. The numbers in the images indicate the angle of inclination, in degrees, of the sun.

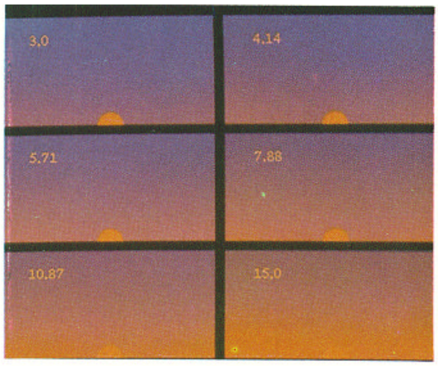

Fig. 8. The effect of variation of haze density (sunset).

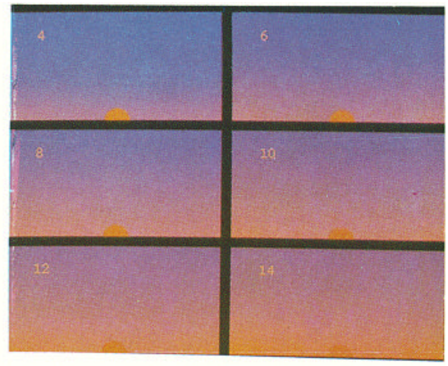

Fig. 9. The effect of variation of haze thickness (sunset).

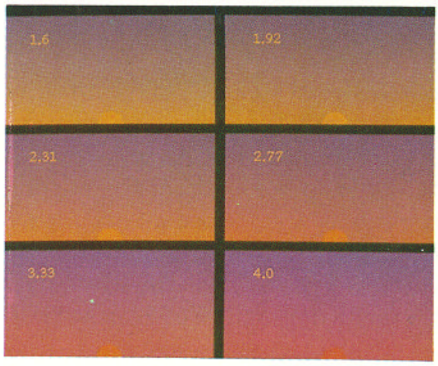

Fig. 10. The effect of variation of air density (sunset).

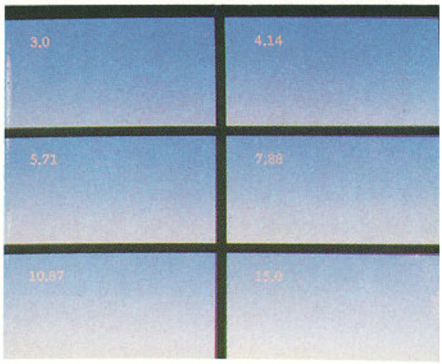

Fig. 11. The effect of variation of haze density (midday).

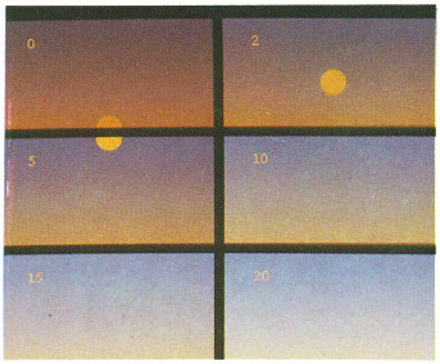

Fig. 12. The effect of variation of solar inclination.

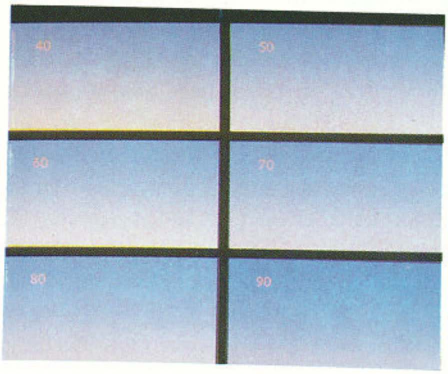

Fig. 13. The effect of variation of solar inclination.

9. LIGHTING CONSIDERATIONS IN THE PRESENCE OF FOG

Scenes containing fog or mist may be divided into the following four classes: The scene may be predominantly lit by the sun, or there may be artificial lighting. The viewer may be in the fog or outside it. In the interests of brevity, only the special case of naturally lit fog will be considered, and even that without shadows. The addition of shadows (specifically shadowed regions of fog) is a more difficult problem that, although it does not require full ray tracing, does require some form of shadow casting.

The prime distinctions between natural and artificial lighting stem from the relative strengths and distances of the sources. Only the sun and the moon deserve consideration, since starlight is too dim to have an effect on a foggy night. The chief difference between light from the sun and that from the moon is the intensity; the angle subtended by the moon in the sky is within 3 percent of that subtended by the sun [5]. Since these sources are so far away, the light from all natural light sources shall be assumed to have parallel rays extending throughout the region of interest (computing penumbrae is a separate problem).

10. SCATTERING DUE TO FOG

Whatever the lighting geometry, the two predominant features of light scattering by fog are wavelength independence and directionality [19]. To say that scattering is wavelength independent is generalizing somewhat; the transition from mist to fog has been identified as the point at which wavelength dependence is lost for the visible part of the spectrum [8]. This happens at a mode radius of roughly 1 μ for visible light; for all higher values, the amount of attenuation of different parts of the visible spectrum varies less than a few percent [20]. An effect that is quite picturesque and a direct result of the directional nature of scattering is the manner in which fog is lit in a wooded area when the sun is low in the sky. Trees cast shadows in the fog itself leaving the appearance of sharply defined holes in the fog. Such holes are visible only when viewed toward the sun; they disappear when one turns around [22]. To model this effect for general light sources requires ray tracing; however, it is worth noting since it cannot be produced without a good lighting model, and has not, to the author's knowledge, been produced to date. Max gives a method based on shadow volumes and radial scan lines [18]. His method is sufficient for single light sources, but hard to generalize to more than one light.

There are two contributions to the color of a pixel: the light reflected by the object that is visible in that direction, and the light scattered in the direction of the eye by the fog along the line of sight. The opacity of the fog depends on the distance to the object being viewed. This is given in eq. (5); for fog the extinction coefficient, β_{ex}, is relatively wavelength independent and varies from 15 km^{-1} to 40 km^{-1}. The angular scattering function, β_{sc}, for fog droplets is much the same as that for wet haze, only more extremely directional.

We now turn our attention to the geometry of naturally lit fog.

11. THE GEOMETRY OF NATURALLY LIT FOG

We assume that the earth is flat. If the sun is not too low in the sky, this approximation gives good results at low cost. A simple case, useful as a test of

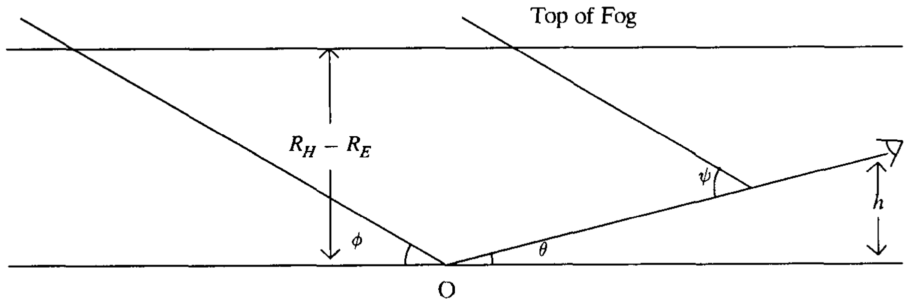

Fig. 14. Lighting in the presence of fog.

the model, has fog of uniform density from the surface of the earth to some constant altitude. For simplicity, R_E will be taken as a constant. For these assumptions the illumination of the ground plane and light reaching the eye from it may be easily derived. With this simple case solved, other cases may be solved by substitution of variables.

To find the color perceived along a particular line of sight, we must consider both the light reflected by any objects along the line of sight, attenuated by the intervening fog, and the light scattered toward the eye by fog along the line of sight. The former component is colored by the reflectance of the object, whereas the latter is the color of the illuminant (here, sunlight). The light scattered toward the eye by fog along the line of sight will be called the *fog* component.

11.1 The Object Component

Consider first the light striking, and hence reflected, from the object (Figure 14). Suppose the top of the fog has the altitude $R_H - R_E$, and the sun is inclined an angle ϕ from the horizontal. An object at O primarily receives light from the sun directly; the intensity of this light is attenuated by a factor depending on the thickness of the fog as measured along a line toward the sun.

$$I = I_0(\exp(-\beta_{ex}t). \tag{34}$$

The thickness is easily derived from the following geometry:

$$t = (R_H - R_E)\csc\phi. \tag{35}$$

A secondary source of light incident on the object is that scattered by fog at some small angle. If specular reflections are not important, the net effect of the light scattered toward the object is to produce a slight increase in the illumination of the surface. It remains to be seen just how important the effect is; for the sake of expediency, we shall introduce an ambient lighting term A to compensate for it.

In eq. (10) we gave the amount of light that reaches the eye from a particular scattering center. Now suppose that a reflecting surface replaces the scattering center. The path the light follows has the same parts as the path used in finding eq. (10): first through clear atmosphere, then through atmosphere containing scattering particles, then a change in direction accompanied by a loss of intensity, and finally through atmosphere containing scattering particles. Clearly eq. (11)

applies here as well. Rather than having an angular scattering coefficient, we need an angular reflectivity coefficient, which will specify the color and angular selectivity of the surface. With the addition of the ambient term, we see a slight change:

$$I_4 = I_0 R^{(\lambda)}(\psi)\exp(-\beta_{\mathrm{ex_m}} d_1 - (d_2 + d_3)(\beta_{\mathrm{ex_m}} + \beta_{\mathrm{ex_p}}))$$

becomes

$$I_4 = \exp(-d_3(\beta_{\mathrm{ex_m}} + \beta_{\mathrm{ex_p}})) \times [A + I_0 R^{(\lambda)}(\psi)\exp(-\beta_{\mathrm{ex_m}} d_1 - (\beta_{\mathrm{ex_m}} + \beta_{\mathrm{ex_p}})d_2)]. \tag{36}$$

The distances d_i are much more easily found than the distances required for computing the color of the sky. First, the distance the light travels before reaching the fog depends only on the thicknesses of the fog and the atmosphere and the angle of inclination of the sun.

$$d_1 = (R_{\mathrm{A}} - R_{\mathrm{H}})\csc \phi. \tag{37}$$

Here some error is introduced in assuming the earth is flat. A careful analysis [14] reveals that the flat-earth approximation is good to within 1 percent for fog, as long as ϕ is not less than 15°.

Since the top of the atmosphere, the top of the fog, and the surface of the earth are all parallel planes, the second distance has much the same form as the first:

$$d_2 = (R_{\mathrm{H}} - R_{\mathrm{E}})\csc \phi. \tag{38}$$

For the distance from the surface to the eye, the angle the line of sight makes with the horizontal is used in the same formula. With the eye at a height h,

$$d_3 = h \csc \theta. \tag{39}$$

With the values of d_i as found above, the light reaching the eye from a source or a reflective object (the *object* component) is

$$I = \exp(-h \csc \theta(\beta_{\mathrm{ex_m}} + \beta_{\mathrm{ex_p}})) \times [A + I_0 R^{(\lambda)}(\psi)\exp(-\csc \phi(\beta_{\mathrm{ex_m}}(R_{\mathrm{A}} - R_{\mathrm{E}}) + \beta_{\mathrm{ex_p}}(R_{\mathrm{H}} - R_{\mathrm{E}})))]. \tag{40}$$

11.2 The Fog Component

To find the fog component, we begin with the assumption that the fog is vertically thin, generally a good assumption, which justifies the approximation of single scattering [10].

To find the amount of light that is scattered toward the eye by fog between the object and the eye, the integral of eq. (11) is used. The distance d_1, that the light travels before reaching the fog is the same as that given in eq. (34). If the viewer is on the ground and the fog layer is not too thin relative to the height of the eye above the ground, then d_2, the distance the light travels through fog before reaching the line of sight, may be approximated as the constant value given in eq. (35). This is equivalent to assuming that no point along the line of sight is far from the ground relative to the height of the fog.

The distance the light travels after striking the line of sight, that is, d_3, varies linearly from 0 to $h \csc \theta$.

The actual value of $\beta_{sc}(\psi)$ is only needed for one angle: $\psi = \theta + \phi$. Substituting the respective distances into eq (12), we find the fog component to be

$$I_f = I_0 \beta_{sc}(\psi) \exp(-\beta_{ex_m}(d_1 + d_2) - \beta_{ex_p} d_2) \int_0^{h\csc\theta} \exp(-d_3(\beta_{ex_m} + \beta_{ex_p}))\, dd_3. \quad (41)$$

The expression may be rewritten as

$$I_f = A(\lambda)\beta_{sc}(\psi) \int_0^{h\csc\theta} e^{-rB(\lambda)}\, dr \quad (42)$$

with

$$B(\lambda) = \beta_{ex_m}^{(\lambda)} + \beta_{ex_p}^{(\lambda)}, \quad (43)$$

$$A(\lambda) = I_0 \exp(-\beta_{ex_m}^{(\lambda)} d_1 - B(\lambda) d_2) \quad (44)$$

$$= I_0 \exp(-\beta_{ex_m}^{(\lambda)} (R_A - R_H)\csc\phi - B(\lambda)(R_H - R_E)\csc\phi).$$

Integrating eq. (42) we have

$$I_f = A(\lambda)\beta_{sc}(\psi) \frac{1 - e^{-B(\lambda)h\csc\theta}}{B(\lambda)}. \quad (45)$$

With the evaluation of the integral solved, the entire expression for I_f may be evaluated using two calls to exp, and some trig functions. The factors that appear outside of the integral need be evaluated only once for a given scene (assuming a constant height ground surface), so the only trig function called for each line of sight is the csc θ that appears in the exponent. Similarly, only one of the two calls to exp is required for each line of sight.

When the sun is at the horizon (either rising or setting), the problem must be treated differently. In this case the distance the sunlight travels through the fog is less than infinite because of the curvature of the earth.

For small solar angles of inclination (such that the curvature of the earth plays a part), no direct light from the sun reaches visible objects (it is all scattered out of the beam). For this reason the best way to model this situation is to use a constant color and intensity for the fog component, to represent the light reaching the fog along the line of sight indirectly. No reflections of the light source are possible, but the ambient lighting will be the same color as the fog component. Both the fog component and the ambient light exist as a result of multiple scattering, predominantly from light striking different parts of the fog directly from the sun. Little absorption takes place as light passes through the fog, but after enough scatterings the direction of propagation is fairly random. Since scattering by fog is nearly wavelength independent, the color of ambient light is nearly the same as the color of direct sunlight without the intervening fog, as is the color of the fog component.

The formulation of the color (and intensity) of the object component took into account the opacity of the fog between the object and the eye. With both components computed, they may be simply added to each other to yield the total light along a particular line of sight.

If the eye is not actually within the fog, the light may be calculated as if the eye were at the point of intersection of the line of sight with the top surface of the fog. This is the same as taking the above integral in which the integrand was weighted with a step function that drops from 1 to 0 at the boundary, the height of this step function being the density of the fog. This ignores any molecular scattering that might occur between the top of the fog and the eye. If the fog is more than a few kilometers from the viewer, the renderer must take into account Rayleigh scattering between the eye and the fog. This may be done by computing the opacity and light contribution of the air between the fog and the eye, and reducing the contribution of the fog and any objects within the fog by an amount that depends on the opacity of the air, while adding to the total light for that line of sight the light scattered toward the eye by the air. The light scattered by the air, and the opacity of the air may be obtained in exactly the same manner as those for the fog component were, substituting in the appropriate scattering and extinction coefficients.

12. EFFICIENCY CONSIDERATIONS FOR NATURALLY LIT FOG

A number of safe assumptions come to our aid here. To begin with, we are not presuming to deal with cases in which the sun is low in the sky. This means that once the light strikes the top of the fog it travels a sufficiently short distance that significant amounts of Rayleigh scattering cannot occur. The fog makes up only a small part of the atmosphere, so the color and intensity of the light striking the top of the fog may be computed (once) as if it were striking the earth, without the fog. This problem was solved when the color of the sun was found.

Since the selectivity of fog is less than 5 percent, and has been measured for red, green, and blue lights, there is no need to compute in wavelength space unless Cook–Torrance shading is being used when reflectances are computed. Assuming 33 wavelengths would have been sampled, this is a saving of a factor of 11 in the time that will be needed to compute the image.

The extinction coefficient of fog $\beta_{\mathrm{ex_p}}$ is much greater than that for air molecules, even though the air molecules are much more densely concentrated [19]. This means that $B(\lambda)$ is effectively $\beta_{\mathrm{ex_p}}$.

If the intensity and color of light reaching the edge of the fog have been computed once and stored in I_t, then eq. (45) becomes

$$I_f = I_t \exp(-\beta_{\mathrm{ex_p}}(R_{\mathrm{H}} - R_{\mathrm{E}})\csc\phi)\beta_{\mathrm{sc}}(\psi)\,\frac{1 - \exp(-\beta_{\mathrm{ex_p}} h \csc\theta)}{\beta_{\mathrm{ex_p}}}. \tag{46}$$

In a similar way, eq. (40) can be rearranged as follows:

$$\begin{aligned} I &= A\exp(-h\csc\theta B(\lambda)) \\ &\quad + R^{(\lambda)}(\psi)I_0\exp[-h\csc\theta B(\lambda) - \beta_{\mathrm{ex_m}}(R_{\mathrm{A}} - R_{\mathrm{H}})\csc\phi \\ &\qquad + B(\lambda)(R_{\mathrm{H}} - R_{\mathrm{E}})\csc\phi] \\ &= A\exp(-h\csc\theta\beta_{\mathrm{ex_p}}) + I_t\exp(-h\csc\theta\beta_{\mathrm{ex_p}} - \beta_{\mathrm{ex_p}}(R_{\mathrm{H}} - R_{\mathrm{E}})\csc\phi)R^{(\lambda)}(\psi). \end{aligned} \tag{47}$$

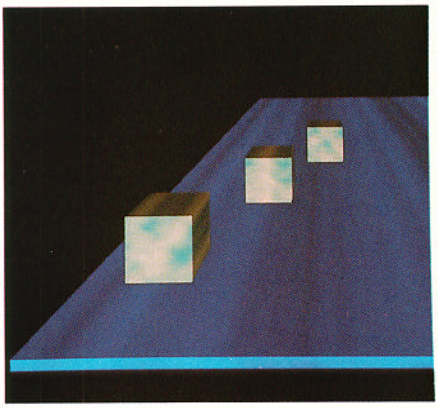

Fig. 15. A simple scene, lit from the front, without fog.

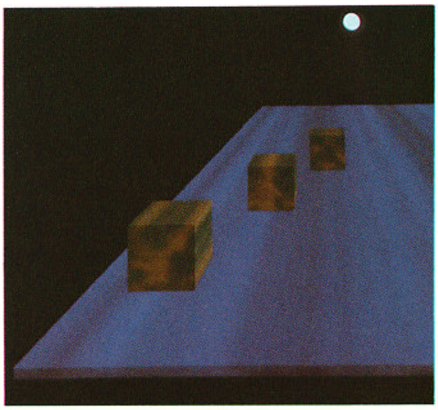

Fig. 16. The same scene, with fog.

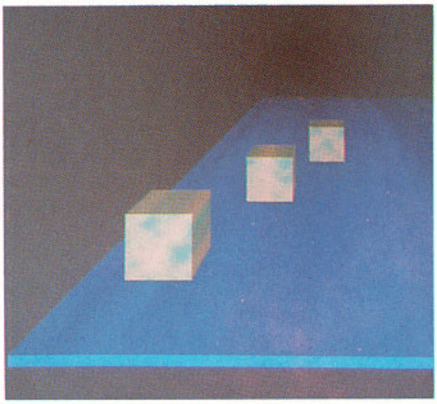

Fig. 17. The same scene, back lit, no fog.

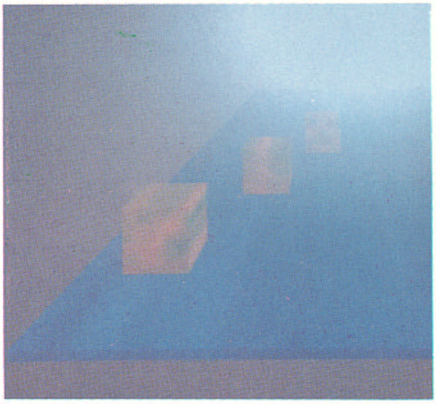

Fig. 18. The same scene, back lit, with fog.

If the exponent in the first term is very large, it is safe to assume that the object is sufficiently obscured by the fog as to make no contribution.

In many cases the fog component is determined solely by the distance from the object to the eye, all other parameters remaining nearly constant throughout an image, and the object component may be computed as if the fog were not there, since its vertical thickness is so small. This is also the case for haze when the sun is well above the horizon. As long as shadows in the fog are not important, there is nothing to prevent a scene from being rendered without fog or haze, with the fog or haze being added later, so long as the distance information is retained. Any rendering algorithm has this information available either implicitly or explicitly and can retain it in a hidden field of the image such as is done in [7].

Figures 15 and 16 show a simple scene lit from the front. In the one case the scene is shown without fog, and in the other it is with fog. Note the lack of light reflected from the fog toward the eye, especially in the center, where light would have to be scattered back nearly on its path. Figures 17 and 18 show the same scene lit from behind. Here the fog scatters considerable light toward the eye, particularly in the region where the light follows a nearly direct path.

13. SUMMARY

Computer-generated imagery has, until now, used ad hoc methods of determining the colors of the sun and sky. With this unified lighting model, the sun, sky, clouds, and even objects on the ground reflecting light from the sun and sky can fit together, being computed from the same lighting parameters. In this way images of outdoor scenes need no longer have the appearance of being pasted together, but rather form one harmonious unit.

The cost of computing a scene in this way is not small; however, some methods of keeping the cost down without sacrificing realism have been discussed.

ACKNOWLEDGMENTS

The work of McCartney [19] supplied an excellent description of the nature and effect of scattering, with a very complete bibliography. Without such a complete reference, this work would have taken much longer. I also wish to thank my master's thesis supervisor, Richard Bartels, for his encouragement and support.

REFERENCES

1. BLINN, J. F. Simulation of wrinkled surfaces. *Comput. Graph. 12*, 3 (Aug. 1978), 286–292.
2. BLINN, J. F. Light reflection techniques for simulation of clouds and dusty surfaces. *Comput. Graph. 16*, 3 (July 1982), 21.
3. BURDEN, R. L., FAIRES, J. D., AND REYNOLDS, A. C. *Numerical Analysis*. Prindle, Weber, and Schmidt, Boston, Mass., 1978.
4. COOK, R. L., AND TORRANCE, K. E. A reflection model for computer graphics. *Comput. Graph. 15*, 3 (Aug. 1981), 307–316.
5. CRC. *Handbook of Chemistry and Physics*. CRC Press, Boca Raton, Fla., 1981.
6. DENMAN, H. H., HELLER, W., AND PANGONIS, W. J. *Angular Scattering Functions of Spheres*. Wayne State University Press, Detroit, Mich. 1966.
7. DUFF, T. Compositing 3-D rendered images. *Comput. Graph. 19*, 3 (July 1985), 41–44.
8. ELDRIDGE, R. G. Mist—The transition from haze to fog. *Bull. Am. Meteorol. Soc. 50*, 6 (June 1969), 422–426.
9. FRITZ, S. Solar radiant energy and its modification by the earth and its atmosphere. In *Compendium of Meteorology*, T. F. Malone, Ed. American Meteorological Society, Boston, Mass., 1951.
10. GEORGE, J. J. Fog. In *Compendium of Meteorology*, T. F. Malone, Ed. American Meteorological Society, Boston, Mass., 1951.
11. GORAL, C. M., TORRANCE, K. E., AND BATTAILE, B. Modeling the interaction of light between diffuse surfaces. *Comput. Graph. 18*, 3 (July 1984), 213–222.
12. GREENE, N. *Comput. Graph. 18*, 3 (July 1984). Caption from cover image.
13. KAJIYA, J., AND VON HERZEN, B. P. Ray tracing volume densities. *Comput. Graph. 18*, 3 (July 1984), 165–173.
14. KLASSEN, R. V. Modelling the effect of scattering—A new lighting model for computer imagery. Master's thesis, Dept. of Computer Science, Univ. of Waterloo, Waterloo, Ontario, Dec. 1985.
15. KLASSEN, R. V., AND BARTELS, R. H. Using B-splines for re-sizing images. Tech. Rep. CS-86-55, Dept. of Computer Science, Univ. of Waterloo, Waterloo, Ontario, 1986.
16. MAX, N. Vectorized procedural models for natural terrain: Waves and islands in the sunset. *Comput. Graph. 15*, 3 (Aug. 1981), 317–324.
17. MAX, N. Light diffusion through clouds and haze. *Comput. Vision, Graph. Image Process. 33*, 3 (Mar. 1986), 280–292.

18. MAX, N. Atmospheric illumination and shadows. *Comput. Graph. 20*, 4 (Aug. 1986), 117–124.
19. MCCARTNEY, E. J. *Optics of the Atmosphere.* Wiley, New York, 1976.
20. MIDDLETON, W. E. K. *Vision through the Atmosphere.* University of Toronto Press, Toronto, Ontario, 1952.
21. MIE, G. Bietage zur Optik truber Medien Speziell Kolloidaler Metallosungen. *Annallen der Physik 25*, 3 (1908), 377.
22. MINNAERT, M. *Light and Colour in the Open Air.* Dover, New York, 1954.
23. PERLIN, K. *A unified reflectance and texturing model. In SIGGRAPH 84 Advanced Image Synthesis Course Notes.* ACM, New York, July 1984.
24. STRUTT, J. W. (Lord Rayleigh). On the light from the sky, its polarization and colour. *Philos. Mag. 41* (Apr. 1871), 107–120, 274–279. Reprinted in Lord Rayleigh, *Scientific Papers, I.* Dover, New York, 1964, pp. 87–103.
25. WHITTED, T. An improved illumination model for shaded display. *Commun. ACM 23*, 6 (June 1980), 343–349.
26. WHITTED, T., AND WEIMER, D. M. *Comput. Graph. 15*, 3 (Aug. 1981). Caption for Figure 6 of back cover.

Received November 1985; revised January 1987; accepted January 1987